Aggregates of the Chlorophyll-Binding Protein IsiA (CP43′) Dissipate Energy in Cyanobacteria†

Janne A. Ihalainen,‡,§ Sandrine D'Haene,‡ Nataliya Yeremenko,|| Henny van Roon,‡ Ana A. Arteni,⊥ Egbert J. Boekema,⊥ Rienk van Grondelle,‡ Hans C. P. Matthijs,|| and Jan P. Dekker*,‡

Division of Physics and Astronomy, Faculty of Sciences, Vrije Universiteit, De Boelelaan 1081, 1081 HV Amsterdam, The Netherlands, Aquatic Microbiology, Institute of Biodiversity and Ecosystem Dynamics, Faculty of Science, Universiteit van Amsterdam, Nieuwe Achtergracht 127, 1018 WS Amsterdam, The Netherlands, and Department of Biophysical Chemistry, Groningen Biomolecular Sciences and Biotechnology Institute, University of Groningen, Nijenborgh 4, 9747 AG Groningen, The Netherlands

Received June 6, 2005; Revised Manuscript Received June 24, 2005

ABSTRACT: In many natural habitats, growth of cyanobacteria may be limited by a low concentration of iron. Cyanobacteria respond to this condition by expressing a number of iron-stress-inducible genes, of which the *isiA* gene encodes a chlorophyll-binding protein known as IsiA or CP43′. IsiA monomers assemble into ring-shaped polymers that encircle trimeric or monomeric photosystem I (PSI), or are present in supercomplexes without PSI, in particular upon prolonged iron starvation. In this report, we present steady-state and time-resolved fluorescence measurements of isolated IsiA aggregates that have been purified from an iron-starved *psaFJ*-minus mutant of *Synechocystis* PCC 6803. We show that these aggregates have a fluorescence quantum yield of ∼2% compared to that of chlorophyll *a* in acetone, and that the dominating fluorescence lifetimes are 66 and 210 ps, more than 1 order of magnitude shorter than that of free chlorophyll *a*. Comparison of the temperature dependence of the fluorescence yields and spectra of the isolated aggregates and of the cells from which they were obtained suggests that these aggregates occur naturally in the iron-starved cells. We suggest that IsiA aggregates protect cyanobacterial cells against the deleterious effects of light.

A daily type of stress experienced by many organisms performing oxygenic photosynthesis is the condition in which the input of light exceeds the rate of carbon fixation (*1*). This condition can lead to the accumulation of excited states of chlorophyll, which in the presence of oxygen can lead to severe damage to the organism. Therefore, all photosynthetic organisms have developed mechanisms by which excess excitation energy can be harmlessly dissipated into heat. This dissipation is manifested as a decrease in the fluorescence quantum yield, and is generally known as nonphotochemical quenching (NPQ).[1] The part of NPQ that is related to rapid fluctuations of the light intensity is known as high-energy quenching or qE (*2*, *3*).

Recent progress has revealed some of the basic features of qE in green plants. The process is triggered by acidification of the thylakoid lumen, which activates the enzyme violaxanthin de-epoxidase, the enzyme that converts the carotenoid violaxanthin into zeaxanthin (*4*). At least in higher plants, qE requires the presence of the PsbS protein and its protonation by the acidification of the thylakoid lumen (*5*, *6*). Also, zeaxanthin (Zea) needs to be activated, possibly by binding to PsbS (*7*, *8*). It was recently postulated (*9*) that the activated Zea forms a heterodimer with a chlorophyll (Chl) molecule, which upon excitation rapidly converts into a charge-separated state (consisting of a Chl anion and a Zea cation) that recombines to the Chl−Zea ground state in ∼150 ps, and thus dissipates the excitation energy. It is likely that the energy transfer to the activated Chl−Zea heterodimer determines the kinetics of the process (*9*). Other mechanisms have also been proposed, such as energy transfer from a chlorophyll, identified in the 2.5 Å structure of the main light-harvesting complex of green plants (LHCII), to the low-lying S1 state of Zea, from which the excitation energy will be dissipated as heat (*10*, *11*). In addition, aggregation of LHCII may give rise to a shorter distance between two Chl molecules (Chl 2 and 7 in ref *11*), which have a shorter excited-state lifetime and therefore can dissipate energy (*12*). It is also possible that the activated Zea induces other conformational changes in the antenna system that are accompanied by an increased rate of dissipation of excitation energy (*2*, *3*). High-energy quenching also occurs in green

† J.A.I. was supported by the European Union (Grant HPRN-CT-2002-00248) and by the Academy of Finland (Project 203824). The work of J.P.D., R.v.G., and E.J.B. was supported by the European Union [Grant MRTN-CT-2003-505069 (Intro2)] and by grants from the Foundation of Life and Earth Sciences (ALW) of the Netherlands Organization for Scientific Research (NWO).

* To whom correspondence should be addressed. Telephone: +31 20 5987931. Fax: +31 20 5987999. E-mail: JP.Dekker@few.vu.nl.

‡ Vrije Universiteit.

§ Present address: Physikalisch Chemisches Institut, Universität Zürich, Winterthurerstrasse 190, CH-8057 Zürich, Switzerland.

|| Universiteit van Amsterdam.

⊥ University of Groningen.

[1] Abbreviations: β-Car, β-carotene; β-DM, *n*-dodecyl β-D-maltoside; Chl, chlorophyll; DAS, decay-associated spectrum; Ech, echinenone; fwhm, full width at half-maximum; IEC, ion-exchange chromatography; Isi, iron stress inducible; NPQ, non-photochemical quenching; PBS, phycobilisome; PSI, photosystem I; PSII, photosystem II; qE, high-energy quenching; Zea, zeaxanthin.

10.1021/bi0510680 CCC: $30.25
Published on Web 07/22/2005

algae (*8*, *13*) and in diatom algae (*14*) and is very pronounced in evergreens, which in freezing conditions are permanently in a highly quenched state (*15*, *16*). It was shown that in green plants NPQ processes can also occur in the absence of zeaxanthin (*12*, *17*) or PsbS (*18*), suggesting that more than one quenching mechanism plays a role in green plants.

Until recently, cyanobacteria were thought to be unable to regulate photosynthesis by an NPQ mechanism. The main regulation mechanism was considered to be the state transition, in which the membrane peripheral phycobilisomes (PBS) move from photosystem II (PSII) to photosystem I (PSI) and back to adjust for imbalances in photosynthetic electron transport (*19*). However, a number of recent experiments suggest that, under special conditions, cyanobacteria can give rise to very pronounced NPQ. It was demonstrated that in a PSII-less mutant of *Synechocystis* PCC 6803 intense blue light gives rise to an ~40% decrease in PBS fluorescence (*20*). Under conditions in which the "iron-stress-inducible" proteins are expressed by the *isiAB* operon [iron depletion or oxidative stress in general (*21*)], a strong NPQ was found (*22*) that also was triggered by blue light (*23*) and that was particularly pronounced after prolonged iron depletion (*24*).

The *isiAB* operon expresses two proteins, IsiA and IsiB. IsiB is flavodoxin, which replaces the iron-rich soluble electron transfer protein ferredoxin. IsiA belongs to the core-complex family of chlorophyll-binding proteins (*25*), which also includes the well-characterized CP47 and CP43 core antenna proteins of PSII. IsiA can build a ring of 18 units around trimeric PSI (*26*, *27*), or of 17 units if the PsaJ and PsaF subunits are missing (*28*). Recent elaborate electron microscopic analyses of supercomplexes prepared from *Synechocystis* PCC 6803 grown under variable degrees of iron depletion revealed that IsiA can also build several other types of rings, such as rings of 12−13 units around monomeric PSI, double rings of up to 35 units around monomeric PSI, PSI with incomplete rings, and the same types of rings but without a photosystem (*29*−*31*). These IsiA-only supercomplexes were particularly abundant in *psaFJ*$^-$ cells, but were also quite abudant in wild-type cells. The "standard" $(PSI)_3(IsiA)_{18}$ complexes have been analyzed by steady-state (*32*) and time-resolved (*33*, *34*) spectroscopic techniques, and it was concluded that in these supercomplexes IsiA efficiently harvests light for PSI. The average time by which excitations become trapped by charge separation in the reaction center was shown to be ~40 ps (*33*, *34*), nearly 2 times longer than in the PSI core complex. On the basis of these findings, it was suggested that the IsiA bound to PSI has a light-harvesting function and that the unconnected IsiA is involved in photoprotection (*29*). The photoprotection function was confirmed and extended by the recent finding that IsiA is, under iron-replete growth conditions, also induced by high light and protects the organism from photooxidative stress (*35*).

In this report, we present steady-state and time-resolved fluorescence measurements of IsiA aggregates isolated from long-term iron-depleted *psaFJ*$^-$ *Synechocystis* cells. The *psaFJ*$^-$ mutant was used because of the relative abundance of IsiA-only supercomplexes over PSI−IsiA supercomplexes. The results indicate that these aggregates contain Chl *a*, β-carotene (β-Car), echinenone (Ech), and Zea as main pigments, and give rise to a very strong quenching of the fluorescence. This indicates that cells with large amounts of IsiA aggregates are in a strongly quenched state.

MATERIALS AND METHODS

Organism and Culture. The *psaFJ*$^-$ mutant of *Synechocystis* sp. PCC 6803 (*21*) was grown at 30 °C in liquid BG11 medium at a light intensity of 50 μmol of photons m^{-2} s^{-1} in ambient air. Iron deficiency was achieved as described previously (*29*). In the work presented here, cells harvested 30−40 days after inoculation were used.

Preparation of IsiA Aggregates. Cells were broken and thylakoid membranes isolated as described previously (*29*). Freshly isolated thylakoid membranes (0.15 mg of Chl *a*/mL) were solubilized with 0.5% (w/v) *n*-dodecyl β-D-maltoside (β-DM) and centrifuged at 9000*g* for 3 min. The supernatant was filtered on a Titan PVDF syringe filter (0.45 μm) and subjected to a MonoQ column (Pharmacia) for ion-exchange chromatography (IEC). The running buffer consisted of 20 mM Bis-Tris (pH 6.5), 10 mM $MgCl_2$, 20 mM NaCl, 15 mM $MgSO_4$, 1.5% taurine, and 0.03% β-DM. A gradient with $MgSO_4$ up to 500 mM was applied. The IsiA aggregates eluted at a $MgSO_4$ concentration of ~250 mM. The IEC was monitored with an on-line diode array detector (Shimadzu SPD-M10Avp). Size-exclusion chromatography was conducted with a Superdex 200 HR 10/30 column (Pharmacia) as described previously (*29*).

Pigment Analysis. Pigment analysis was performed according to the method of Gilmore et al. (*36*). For this procedure, pigments were extracted with 80% acetone, centrifuged, and loaded on a RP-HPLC column (Lichrosorb C18, 10 μm, 250 mm × 4.6 mm), which was equilibrated in buffer A [85% acetonitrile, 13.5% methanol, and 1.5% 0.2 M Tris-HCl (pH 8.0)]. After a 15 min isocratic run with a flow rate of 1 mL/min, myxoxanthophyll, zeaxanthin, and an unknown carotenoid were eluted from the column. After a linear gradient of 3 min to buffer B (83.3% methanol and 16.7% *n*-hexane) and an isocratic run for 40 min with buffer B, chlorophyll *a*, echinenone, and β-carotene were eluted. The HPLC system was equipped with a diode-array optical absorption spectrophotometer, which allowed identification of the peaks in the chromatogram by their absorption spectra.

Electron Microscopy. EM was performed as described in ref *29*. Briefly, EM specimens were prepared on glow-discharged carbon-coated grids, using 2% uranyl acetate as a negative stain, and EM was performed on a Philips EM120 electron microscope. Images were recorded with a Gatan 4000 SP 4K slow-scan camera at 46900× magnification with a pixel size (without binning the images) of 3.2 Å at the specimen level.

Steady-State Emission. Room-temperature emission spectra were measured with a commercial spectrophotometer (Jobin Yvon, Fluorolog), with 430 nm excitation (bandwidth of 3 nm) and detection with 1 nm resolution. The absorbance of the sample was 0.1 at 680 nm. For low-temperature measurements, the isolated aggregates were diluted in 20 mM Bis-Tris (pH 6.5), 20 mM NaCl, 0.06% β-DM, and 66% (v/v) glycerol to an absorbance of 0.1 at 680 nm and cooled in a helium-bath cryostat, which allowed a temperature range of 4.2−230 K. The cells were diluted in 20 mM Bis-Tris (pH 6.5) and 5 mM $MgCl_2$ to an OD_{680} value of 0.1. Fluorescence emission spectra were measured with a $^1/_2$ m

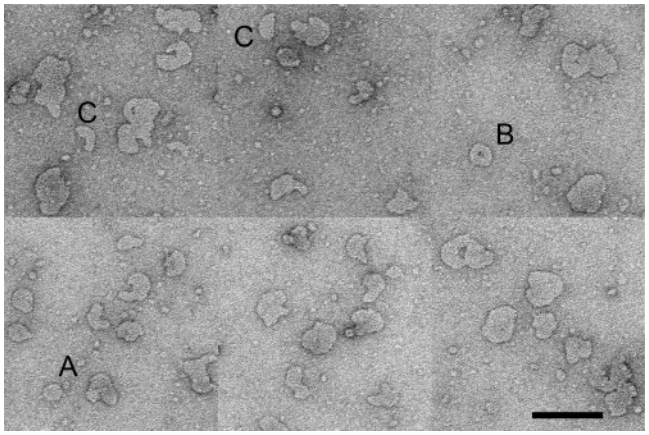

FIGURE 1: Selected parts from electron micrographs showing IsiA aggregates of variable size. A PSI complex with a single IsiA ring (marked A), an IsiA complex with a double ring (marked B), and some incomplete rings (marked C) have been indicated. The bar is 100 nm.

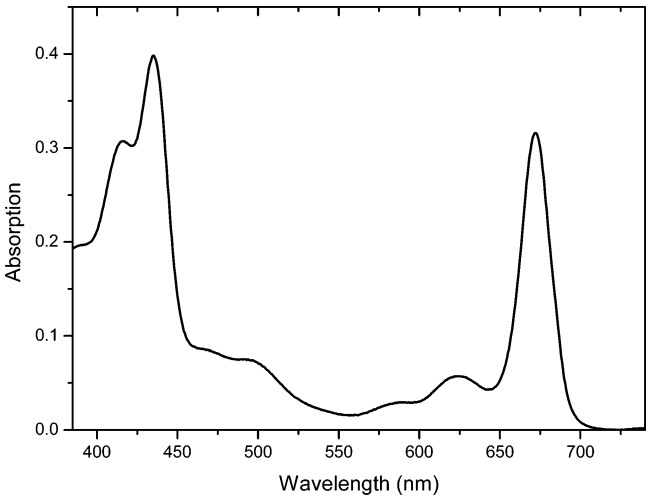

FIGURE 2: Absorption spectrum of isolated IsiA aggregates at room temperature.

imaging spectrograph and a CCD camera (Chromex Chromcam I). The spectral resolution was ~0.5 nm. For broadband excitation, a tungsten halogen lamp (Oriel) was used with band-pass filters transmitting at 420 nm (bandwidth of 20 nm). The obtained emission spectra were corrected for the wavelength-dependent sensitivity of the detection system.

Time-Resolved Emission. Time-resolved emission measurements were performed with a Streak camera setup. The sample was placed into a 2 mm thick spinning cell with a diameter of 10 cm and a rotation speed of 33 Hz. The absorbance of the sample was 0.12 at 680 nm. Excitation pulses of 400 nm (~100 fs) with vertical polarization were generated using a titanium:sapphire laser (Coherent, VITESSE) with a regenerative amplifier (Coherent, REGA), a double-pass optical parametric amplifier (Coherent, OPA), and a Berek compensator. The repetition rate was 150 kHz with a pulse energy of 0.23 nJ in the sample, which resulted in ~0.05% excited chlorophylls per pulse. The fluorescence was detected at a right angle with respect to the excitation beam through a polarizer at the magic angle, using a Chromex 250IS spectrograph and a Hamamatsu C5680 synchroscan streak camera. The streak images were recorded with a cooled Hamamatsu C4880 CCD camera. The detected streak images were analyzed globally, and the estimated decay-associated spectra (DAS) were determined (*37*, *38*). Two time bases of the instrument were used, and the instrument response functions were modeled as Gaussians with fwhm values of ~6 and ~24 ps. The wavelength resolution of the experiment was ~8 nm.

RESULTS

Pigment Composition and Structure of Isolated IsiA Aggregates. We used ion-exchange chromatography to purify β-DM-solubilized IsiA aggregates from long-term iron-depleted *psaFJ*$^-$ *Synechocystis* sp. PCC 6803 cells. Gel filtration experiments revealed that the isolated fraction consisted of very large complexes and was essentially free of monomeric IsiA (data not shown). Figure 1 shows EM micrographs of the isolated fraction. In agreement with earlier EM experiments on supercomplexes from long-term iron-depleted *Synechocystis* cells (*29*, *31*), complete and incomplete double rings of IsiA were visible, though in this particular case relatively many even larger aggregates with variable size and shape were formed. We found that the isolated aggregates are very stable, and that incubation with 0.5% β-DM and 2 M $LiClO_4$ did not induce the release of monomeric IsiA. The same treatment effectively removed the sequence-related CP43 protein from the PSII core complex (*39*). Figure 2 shows the room-temperature absorption spectrum of the isolated aggregates. The Q_y absorption maximum of the chlorophylls peaks at 672 nm, and the carotenoids have absorption maxima around 496 and 470 nm.

Table 1: Pigment Composition of Purified IsiA Aggregates, Normalized to a Content of 16 Chl *a* Molecules per Monomer

pigment	no. per complex	pigment	no. per complex
chlorophyll *a*	16.0	zeaxanthin	0.7
β-carotene	1.9	unknown	0.2
echinenone	1.0	myxoxanthophyll	0.1

Pigment analysis revealed the presence of four major types of pigments, i.e., Chl *a*, β-Car, Zea, and echinenone (Ech), as well as some impurities (Table 1). If each IsiA protein binds 16 Chl *a* molecules (*32*), then it probably also binds two β-Car molecules, one Zea molecule, and one Ech molecule. These results indicate that the IsiA protein differs from the related CP43 protein of green plants by the binding of zeaxanthin and echinenone. We note that both carotenoids are rather common in cyanobacterial membranes, that small amounts of Zea were also detected in purified PSII core preparations from *Synechocystis* (*40*), and that Ech is the carotenoid bound to the cytochrome b_6f complex of *Synechocystis* (*41*).

Temperature Dependence of Steady-State Emission. Figure 3 shows 4.2 K emission spectra of the isolated IsiA aggregates (solid line), *Synechocystis* cells grown for 40 days in iron-free medium (dotted line), and *Synechocystis* cells grown in the presence of iron (dashed line). The IsiA aggregates show a narrow (fwhm = 6.8 nm) emission band peaking at 686.9 nm, accompanied with vibrational transitions at longer wavelengths. This spectrum is virtually identical with that of the *Synechocystis* cells from which the aggregates were obtained, and demonstrates the absence of PSI in this preparation. However, PSI emission around 720 nm dominates the spectrum of *Synechocystis* cells grown with

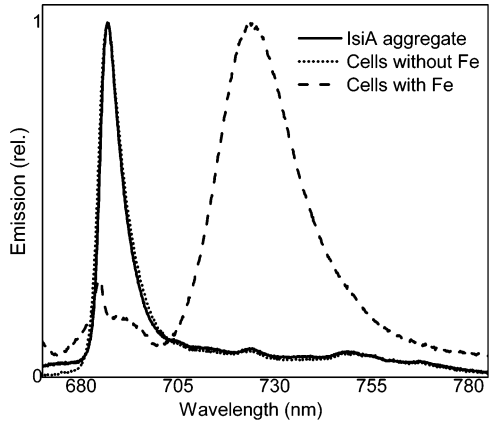

FIGURE 3: Fluorescence emission spectra at 4.2 K upon 420 nm excitation of the isolated IsiA aggregates (—), *psaFJ*-depleted *Synechocystis* 6803 cells grown for 40 days without iron (•••), and wild-type *Synechocystis* 6803 cells grown in the presence of iron (- - -). All spectra were normalized to their maxima.

iron (Figure 3), whereas IsiA emission is nearly absent. The temperature dependence of the emission of the isolated IsiA aggregates between 4.2 and 230 K is shown in Figure 4A. The most striking effect of the temperature dependence of the fluorescence of the IsiA aggregates is a strong decrease in the total emission yield with an increase in temperature (Figure 4C). A similar behavior, albeit not as strong as presented here, was observed with large three-dimensional LHCII aggregates (*42*), though in the LHCII aggregates the decrease in yield with an increase in temperature was accompanied by a clear red shift of the fluorescence, whereas in IsiA aggregates a small blue shift of the peak position occurs (Figure 4D). Figure 4B demonstrates that in intact cells a similar temperature dependence of the fluorescence occurs, indicating that the observed effect is not a result of the purification procedure of the aggregates and occurs as such in the cells. Figure 4C shows that the decrease in emission yield is even slightly stronger in the intact cells, and that the emission yield at 240 K is only 6% of that at 4.2 K. The difference with the isolated aggregates originates probably mostly from a small contamination of unconnected chlorophylls in the isolated aggregates. At 4.2 K, the free chlorophyll emission is seen as a small shoulder at ~673 nm (Figure 4A). Although the amount of the free pigments is at most 2−3% in the preparation, their effect on the overall emission spectrum of the preparation becomes more prominent at elevated temperatures, as the excitation lifetime of the IsiA aggregates becomes ultimately shorter (see below) and the lifetime of free chlorophylls remains basically constant (~5 ns) at all temperatures. We note that the PSI core complex of *Synechocystis* 6803 exhibits a very moderate temperature dependence of the emission yield between 4 and 77 K (*43*). Only at higher temperatures are excitations able to escape from the "red" chlorophylls and thus give rise to photochemical quenching by trapping in the reaction center.

Steady-State Emission at Room Temperature. Figure 5 shows a comparison between the room-temperature emission spectra of the isolated IsiA aggregates (solid) and of Chl *a* in acetone (dashed). The emission maximum of the IsiA aggregates is located at 679 nm, and the emission band is slightly wider (23.8 nm) than that of Chl *a* in acetone (20 nm), which most likely originates from more than one emitting species (see below). Most strikingly, the integrated emission yield of the IsiA aggregate preparation is only ~4% compared to that of Chl *a* in acetone, as demonstrated in the inset of Figure 5, where the emission spectra are normalized to the same amount of absorbed photons. By comparing the emission values at 675 and 686 nm from the 4.2 K emission spectra (Figure 4A), we estimate that the preparation consists of 2−3% unconnected Chl *a* molecules. These unconnected Chl *a* molecules will contribute ~50% to the room-temperature emission spectrum if the average decay lifetime of the IsiA aggregates is 144 ps (see below) and that of unconnected Chl *a* is ~5 ns. This implies that the IsiA aggregates have an emission yield of 2% compared to that of Chl *a* molecules in acetone. To our knowledge, this is the smallest quantum yield observed in any naturally occurring chlorophyll-containing light-harvesting protein in the absence of reaction centers.

Time-Resolved Emission. To analyze the strong quenching character of IsiA aggregates at room temperature, we performed time-resolved fluorescence measurements with a Streak camera setup. The time-resolved fluorescence signal, obtained at all emitting wavelengths after ultra-short 400 nm excitation pulses, was analyzed globally. This procedure resulted in so-called decay-associated spectra (DAS) with corresponding decay lifetimes. For a proper description of the decaying emission signal, a six-component fit appeared to be necessary (Figure 6). The sub-picosecond spectrum (thin solid line in Figure 6) describes the rise of the emitting states. The first decay component has a lifetime of 9 ps, an integrated decay amplitude of ~7%, and a spectrum with maximum at ~685 nm (dotted line). Then, two main decay lifetimes of 66 ps (dashed line) and 210 ps (solid line) are observed with basically identical spectra. These decay components have integrated decay amplitudes of 36 and 55% of the total excitation decay, respectively, and peak at ~682 nm. Thus, these three components contribute to ~98% of the total excitation decay of the preparation; i.e., these are the decay lifetimes of the IsiA aggregates. The average decay lifetime of the aggregates is then as short as 144 ps. By comparing this number with the decay lifetime of Chl *a* molecules in acetone of 6.1 ns (*44*, *45*), we conclude that IsiA aggregates have an ~50 times faster average decay lifetime than Chl *a* in acetone and should therefore have an emission yield of ~2% compared to that of Chl *a* in acetone.

In addition to the main decay phases, a small long-decaying component with a lifetime of ~2 ns and one subfractional decay component with a lifetime of ~20 ns can be seen. The former component can be assigned to emission from unconnected chlorophyll molecules, and the origin of the latter component is unclear. We also performed fluorescence lifetime experiments on the membranes from which the IsiA aggregates are the dominating chlorophyll-based protein complex, and observed that the main decay lifetimes remain more or less the same (62 and 222 ps) when the aggregates are embedded in the membrane (data not shown).

DISCUSSION

The results presented here show that IsiA aggregates have strikingly short fluorescence lifetimes. To the best of our knowledge, the average decay lifetime of 144 ps belongs to the fastest lifetimes found for any naturally occurring chlorophyll-containing antenna system. Isolated LHCII has

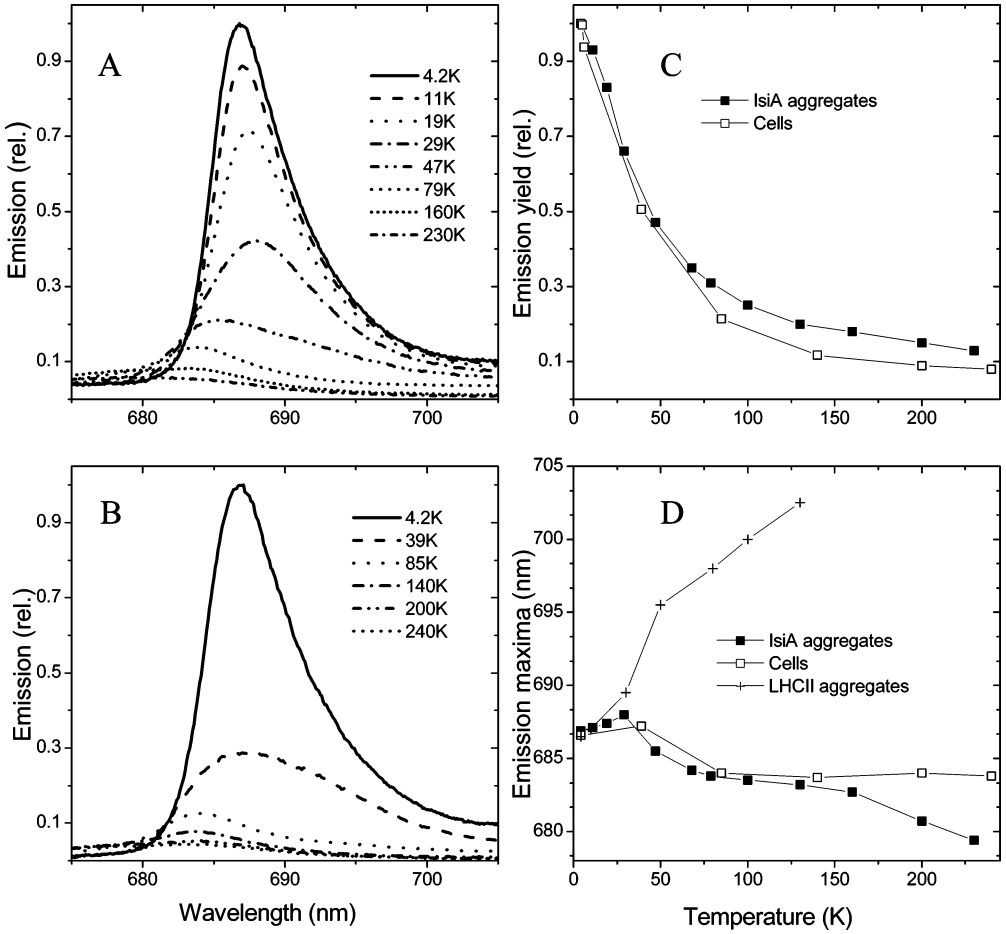

FIGURE 4: Temperature dependence of fluorescence emission. (A) Temperature dependence of the main fluorescence emission band of IsiA aggregates at various temperatures upon 420 nm excitation. (B) Temperature-dependent emission spectra of the main band of *psaFJ*-less *Synechocystis* PCC 6803 cells after iron depletion for 40 days upon 420 nm excitation. (C) Integrated emission intensities as a function of temperature of IsiA aggregates (■) and the *Synechocystis* cells from which the aggregates were obtained (□). The integration interval was from 655 to 815 nm. (D) Maxima of the fluorescence emission peaks of IsiA aggregates (■), *Synechocystis* cells grown for 40 days in Fe-deficient medium (□), and large LHCII aggregates (+, data from ref *42*).

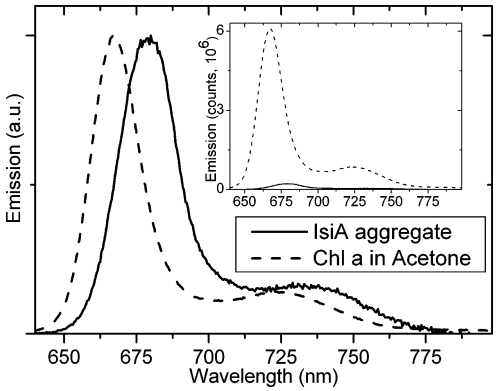

FIGURE 5: Room-temperature emission spectra of IsiA aggregates (—) and Chl *a* in acetone (- - -), normalized to their emission maxima. In the inset, the spectra are normalized to the same amount of absorbed photons; i.e., the emission yields are comparable.

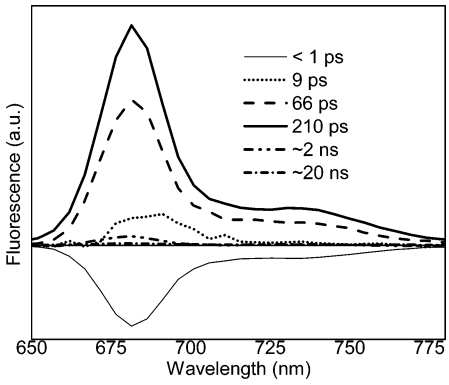

FIGURE 6: Decay-associated spectra (DAS) of the fluorescence decay of IsiA aggregates at room temperature after 400 nm short pulse excitation. The initial spectrum (~1 ps), which stands for the overall rise of the emitting states, is multiplied by a factor of 0.2 for a better view of the other components.

a decay lifetime of ~4 ns (*45*, *46*), whereas large three-dimensional aggregates can have lifetimes as short as 110 ps (*46*), though the latter aggregates are extremely large and artificial and do not occur as such in plant cells. Smaller LHCII aggregates have intermediate lifetimes of, for example, 700 ps (*47*).

The question of whether the previous conclusion that IsiA acts as a light-harvesting antenna in standard $(PSI)_3(IsiA)_{18}$ supercomplexes would have to be modified because of the short excited-state lifetimes of the choropylls in the IsiA aggregates arises. In these complexes, a 40 ps phase was interpreted as the time needed to trap excitation energy by charge separation in the PSI reaction center (*33*, *34*). If in these complexes the excitation energy would also disappear in 144 ps ($k_q = 1/144$ ps^{-1}), then the observed 40 ps phase would be the result of a competition of decay by charge

separation and by dissipation in the antenna ($k = k_q + k_t = 1/40\ ps^{-1}$). The real trapping by charge separation (k_t) would then occur in $1/53\ ps^{-1}$ for 75% of the excitations. However, it is likely that the excitated-state lifetime without charge separation will be considerably longer than 144 ps, because this lifetime is expected to be larger in the PSI core antenna, and because the IsiA aggregate size is much smaller in the $(PSI)_3(IsiA)_{18}$ supercomplex than in the IsiA aggregates shown in Figure 1. In LHCII, smaller aggregates exhibited longer lifetimes (*46*, *47*), so it is expected that smaller IsiA aggregates also exhibit longer lifetimes. This suggests that the previous conclusion (*33*, *34*) about the light-harvesting function of IsiA in $(PSI)_3(IsiA)_{18}$ supercomplexes is justified. In complexes with much larger amounts of IsiA, such as the $(PSI)_1(IsiA)_{31-35}$ supercomplexes (*29*), a significant part of the excitation energy will probably not be used for light harvesting.

Our results do not allow firm conclusions about the mechanism by which the energy is dissipated in IsiA aggregates. A mechanism based on a closer association of two or more Chl molecules in IsiA upon aggregation, as proposed for LHCII aggregates (*11*, *12*), is however unlikely because the closer connection of Chls usually results in increased excitonic interaction and a red shift of the optical transition. In LHCII, aggregation is indeed accompanied by a red shift of the absorption, and is manifested by a very pronounced temperature-dependent red shift of the emission (*42*). In IsiA aggregates, however, there is only an ~1 nm red shift of the emission upon warming from 4 to 30 K (Figure 4D). A mechanism based on energy transfer from chlorophylls to a low-lying S1 state of one of the carotenoids is possible, because all carotenoids in the IsiA aggregates have 11 (β-Car and Zea) or 12 (Ech) conjugated double bonds, and thus may have S1 states with energies lower than that of Chl *a*. Also, a charge transfer mechanism as detected between Zea and Chl in green plants (*9*) is possible. It is possible that the quenching carotenoid is located between IsiA subunits, either between units within a ring or between rings, because monomeric IsiA exhibits a normal temperature dependence of the emission (*32*) and thus dissipates energy to a much smaller extent at higher temperatures. That the quenching originates from a cofactor other than a carotenoid molecule cannot at this stage be ruled out. *Synechocystis* cells in which the Phe181 residue of the D2 protein was substituted with Trp displayed a quenching that was explained by a Trp−Chl charge separation (*48*). The single chlorophyll *a* molecule in the cytochrome b_6f complex has an unusually short lifetime (*49*, *50*) that in view of the high-resolution X-ray structure (*51*) can now be explained by a Tyr−Chl charge separation reaction (*50*). A Trp−Chl or Tyr−Chl charge transfer mechanism could in principle also play a role in the quenching mechanism of IsiA aggregates.

We note that IsiA aggregates do not explain the blue light-induced NPQ observed in *Synechocystis* PCC 6803 (*23*). The temperature-dependent quenching of steady-state fluorescence was in the long-term iron-depleted cells (Figure 4B) nearly identical with blue light and red light excitation (not shown). The cells investigated in ref *23* were probably in a much earlier stage of iron depletion, in view of the reported 77 K fluorescence emission data, and thus in a different state with smaller amounts of IsiA than in our study. This suggests the existence of another NPQ mechanism, triggered by blue light, in early stages of iron depletion. It is possible that this mechanism is related to the blue light-induced quenching of PBS fluorescence observed by Karapetyan and co-workers (*20*). Recent experiments indicate that the water-soluble orange carotenoid protein (OCP) is involved in this mechanism (D. Kirilovsky, personal communication).

It is likely that the extent of iron starvation experienced by the *Synechocystis* cells used in this study is stronger than that usually experienced by cyanobacteria in their natural habitats. However, because the *isiAB* operon is also expressed by high light (*35*) or other types of oxidative stress (*21*), the state of the cells studied here may not be so unnatural (apart from the PsaFJ deletion) that they never can exist as such in nature. Furthermore, iron supply to the Southern Atlantic Ocean relies on occasional sand storms (*52*, *53*), which supports our experimental design with long-term iron-starved cells. Why then do these types of cells accumulate such massive amounts of IsiA that other chlorophyll-containing systems are not seen at all in low-temperature emission spectra of cells? In earlier stages of iron depletion, IsiA surely harvests light for PSI (*32*, *33*), and perhaps also for PSII (*23*), though a direct connection between PSII and IsiA was never reported for *Synechocystis* PCC 6803. However, when IsiA units occur as such in the membranes (without being bound to PSI), then they may very well transfer their energy to PSII, especially when the IsiA aggregate size is not very large and the excited-state lifetimes are longer than those found for the large aggregates studied in Figure 6. Both PSII and IsiA occur in the same membrane, and can in theory be located in the same domains, also because IsiA was found to be quite mobile in cyanobacterial membranes (*54*). In grana from higher plants, more than half of the LHCII population is not directly bound to PSII in PSII−LHCII supercomplexes, but nevertheless, this population also contributes to the light harvesting of PSII (*55*).

In more severe iron depletion stress or other types of oxidative stress, photoprotection will be the main function of IsiA. The shortening of the fluorescence lifetimes of large IsiA aggregates will decrease the rate of energy transfer to PSI (in PSI−IsiA supercomplexes), and also to PSII if IsiA harvests light for PSII under mild iron depletion stress, and thus protects these photosystems against photodamage. This situation is similar to that in green plants under qE conditions. Even further iron depletion will result in membranes in which IsiA is by far the most dominant chlorophyll protein, and it seems that under these conditions, when photosynthesis is almost impossible, the cells are in a permanently quenched state, similar to that of evergreens in freezing temperatures in the winter (*15*). Also, these organisms stay green, and cope with the deleterious effects of light by expressing large amounts of PsbS and thus keep the membranes in a permanently quenched state. So the basic function of IsiA accumulation in cyanobacteria might be to protect the cells against light, but at the same time to keep the cells green so that they can resume growth again as soon as the stress condition is relieved.

REFERENCES

1. Külheim, C., Ågren, J., and Jansson, S. (2002) Rapid regulation of light harvesting and plant fitness in the field, *Science 297*, 91−93.

2. Holt, N. E., Fleming, G. R., and Niyogi, K. K. (2004) Toward an understanding of the mechanism of nonphotochemical quenching in green plants, *Biochemistry 43*, 8281−8289.
3. Horton, P., and Ruban, A. (2005) Molecular design of the photosystem II light-harvesting antenna: Photosynthesis and photoprotection, *J. Exp. Bot. 56*, 365−373.
4. Demmig-Adams, B., and Adams, W. W., III (1996) The role of xanthophylls cycle carotenoids in the protection of photosynthesis, *Trends Plant Sci. 1*, 21−26.
5. Li, X.-P., Björkman, O., Shih, C., Grossman, A. R., Rosenquist, M., Jansson, S., and Niyogi, K. K. (2000) A pigment-binding protein essential for regulation of photosynthetic light harvesting, *Nature 403*, 391−395.
6. Niyogi, K. K., Li, X.-P., Rosenberg, V., and Jung, H.-S. (2005) Is PsbS the site of non-photochemical quenching in photosynthesis? *J. Exp. Bot. 56*, 375−382.
7. Aspinall-O'Dea, M., Wentworth, M., Pascal, A., Robert, B., Ruban, A., and Horton, P. (2002) *In vitro* reconstitution of the activated zeaxanthin state associated with energy dissipation in plants, *Proc. Natl. Acad. Sci. U.S.A. 99*, 16331−16335.
8. Robert, B., Horton, P., Pascal, A. A., and Ruban, A. V. (2004) Insight into the molecular dynamics of plant light-harvesting proteins *in vivo*, *Trends Plant Sci. 9*, 385−390.
9. Holt, N. E., Zigmantas, D., Valkunas, L., Li, X.-P., Niyogi, K. K., and Fleming, G. R. (2005) Carotenoid cation formation and the regulation of photosynthetic light harvesting, *Science 307*, 433−436.
10. Liu, Z., Yan, H., Wang, K., Kuang, T., Zhang, J., Gui, L., An, X., and Chang, W. (2004) Crystal structure of spinach light-harvesting complex at 2.72 Å resolution, *Nature 428*, 287−292.
11. Standfuss, J., Terwisscha van Scheltinga, A. C., Lamborghini, M., and Kühlbrandt, W. (2005) Mechanisms of photoprotection and nonphotochemical quenching in pea light-harvesting complex at 2.5 Å resolution, *EMBO J. 24*, 919−928.
12. Horton, P., Ruban, A. V., Rees, D., Pascal, A., Noctor, G. D., and Young, A. (1991) Control of the light-harvesting function of chloroplast membranes by the proton concentration in the thylakoid lumen: Aggregation states of the LHCII complex and the role of zeaxanthin, *FEBS Lett. 292*, 1−4.
13. Niyogi, K. K., Björkman, O., and Grossman, A. R. (1997) *Chlamydomonas* xanthophylls cycle mutants identified by video imaging of chlorophyll fluorescence quenching, *Plant Cell 9*, 1369−1380.
14. Ruban, A. V., Lavaud, J., Rousseau, B., Gugliemi, G., Horton, P., and Etienne, A.-L. (2004) The super-excess energy dissipation in diatom algae: Comparative analysis with higher plants, *Photosynth. Res. 82*, 165−175.
15. Gilmore, A. M., and Ball, M. C. (2000) Protection and storage of chlorophyll in overwintering evergreens, *Proc. Natl. Acad. Sci. U.S.A. 97*, 11098−11101.
16. Öquist, G., and Huner, N. P. A. (2003) Photosynthesis of overwintering evergreens, *Annu. Rev. Plant Biol. 54*, 329−355.
17. Finazzi. G., Johnson, G. N., Dall'Osto, L., Joliot, P., Wollman, F.-A., and Bassi, R. (2004) A zeaxanthin-independent nonphotochemical quenching mechanism localized in the photosystem II core complex, *Proc. Natl. Acad. Sci. U.S.A. 101*, 12375−12380.
18. Dall'Osto, L., Caffarri, S., and Bassi, R. (2005) A mechanism of nonphotochemical energy dissipation, independent from PsbS, revealed by a conformational change in the antenna protein CP26, *Plant Cell 17*, 1217−1232.
19. Mullineaux, C. W. (1999) The thylakoid membranes of cyanobacteria: Structure, dynamics and function, *Aust. J. Plant Physiol. 26*, 671−677.
20. Rakhimberdieva, M. G., Stadnichuk, I. N., Elanskaya, I. V., and Karapetyan, N. V. (2004) Carotenoid-induced quenching of the phycobilisome fluorescence in photosystem II-deficient mutant of *Synechocystis* sp., *FEBS Lett. 574*, 85−88.
21. Jeanjean, R., Zuther, E., Yeremenko, N., Havaux, M., Matthijs, H. C. P., and Hagemann, M. (2003) A photosystem I *psaFJ-null* mutant of the cyanobacterium *Synechocystis* PCC 6803 expresses the *isiAB* operon under iron replete conditions, *FEBS Lett. 549*, 52−56.
22. Sandström, S., Park, Y. I., Öquist, G., and Gustafsson, P. (2001) CP43′, the isiA gene product, functions as an excitation energy dissipator in the cyanobacterium *Synechococcus* sp PCC 7942, *Photochem. Photobiol. 74*, 431−437.
23. Cadoret, J.-C., Demoulière, R., Lavaud, J., van Gorkom, H. J., Houmard, J., and Etienne, A.-L. (2004) Dissipation of excess energy triggered by blue light in cyanobacteria with CP43′ (*isiA*), *Biochim. Biophys. Acta 1659*, 100−104.
24. Bailey, S., Mann, N. H., Robinson, C., and Scanlan, D. J. (2005) The occurrence of rapidly reversible non-photochemical quenching of chlorophyll *a* fluorescence in cyanobacteria, *FEBS Lett. 579*, 275−280.
25. Green, B. R. (2003) The evolution of light-harvesting antennas, in *Light-Harvesting Antennas in Photosynthesis* (Green, B. R., and Parson, W. W., Eds.) pp 129−168, Kluwer Academic Publishers, Dordrecht, The Netherlands.
26. Bibby, T. S., Nield, J., and Barber, J. (2001) Iron deficiency induces the formation of an antenna ring around trimeric photosystem I in cyanobacteria, *Nature 412*, 743−745.
27. Boekema, E. J., Hifney, A., Yakushevska, A. E., Piotrowski, M., Keegstra, W., Berry, S., Michel, K. P., Pistorius, E. K., and Kruip, J. (2001) A giant chlorophyll-protein complex induced by iron-deficiency in cyanobacteria, *Nature 412*, 745−748.
28. Kouril, R., Yeremenko, N., D'Haene, S., Yakushevska, A. E., Keegstra, W., Matthijs, H. C. P., Dekker, J. P., and Boekema, E. J. (2003) Photosystem I trimers from *Synechocystis* PCC 6803 lacking the PsaF and PsaJ subunits bind an IsiA ring of 17 units, *Biochim. Biophys. Acta 1607*, 1−4.
29. Yeremenko, N., Kouril, R., Ihalainen, J. A., D'Haene, S., van Oosterwijk, N., Andrizhiyevskaya, E. G., Keegstra, W., Dekker, H. L., Hagemann, M., Boekema, E. J., Matthijs, H. C. P., and Dekker, J. P. (2004) Supramolecular organization and dual function of the IsiA chlorophyll-binding protein in cyanobacteria, *Biochemistry 43*, 10308−10313.
30. Kouril, R., Yeremenko, N., D'Haene, S., Oostergetel, G. T., Matthijs, H. C. P., Dekker, J. P., and Boekema, E. J. (2005) Supercomplexes of IsiA and photosystem I in a mutant lacking subunit PsaL, *Biochim. Biophys. Acta 1706*, 262−266.
31. Kouril, R., Arteni, A. A., Lax, J., Yeremenko, N., D'Haene, S., Rögner, M., Matthijs, H. C. P., Dekker, J. P., and Boekema, E. J. (2005) Structure and functional role of supercomplexes of IsiA and photosystem I in cyanobacterial photosynthesis, *FEBS Lett. 579*, 3253−3257.
32. Andrizhiyevskaya, E. G., Schwabe, T. M. E., Germano, M., D'Haene, S., Kruip, J., van Grondelle, R., and Dekker, J. P. (2002) Spectroscopic properties of PSI−IsiA supercomplexes of the cyanobacterium *Synechococcus* PCC 7942, *Biochim. Biophys. Acta 1556*, 265−272.
33. Melkozernov, A. N., Bibby, T. S., Lin, S., Barber, J., and Blankenship, R. E. (2003) Time-resolved absorption and emission show that the CP43′ antenna ring of iron-stressed *Synechocystis* sp. PCC 6803 is efficiently coupled to the photosystem I reaction center core, *Biochemistry 42*, 3893−3903.
34. Andrizhiyevskaya, E. G., Frolov, D., van Grondelle, R., and Dekker, J. P. (2004) Energy transfer and trapping in the photosystem I complex of *Synechococcus* PCC 7942 and in its supercomplex with IsiA, *Biochim. Biophys. Acta 1656*, 104−113.
35. Havaux, M., Guedeney, G., Hagemann, M., Yeremenko, N., Matthijs, H. C. P., and Jeanjean, R. (2005) The chlorophyll-binding protein IsiA is inducible by high light and protects the cyanobacterium *Synechocystis* PCC6803 from photooxidative stress, *FEBS Lett. 579*, 2289−2293.
36. Gilmore, A. N., and Yamamoto, H. Y. (1991) Resolution of lutein and zeaxanthin using a non-endcapped, lightly carbon-loaded C-18 high-performance liquid-chromatographic column, *J. Chromatogr. 543*, 137−145.
37. Holzwarth, A. R. (1996) Data analysis of time-resolved measurements, in *Biophysical Techniques in Photosynthesis* (Amesz, J., and Hoff, A. J., Eds.) pp 75−92, Kluwer Academic Publishers, Dordrecht, The Netherlands.
38. Van Stokkum, I. H. M., Larsen, D. S., and van Grondelle, R. (2004) Global and target analysis of time-resolved spectra, *Biochim. Biophys. Acta 1657*, 82−104.
39. Ghanotakis, D. F., De Paula, J. C., Demetriou, D. M., Bowlby, N. R., Petersen, J., Babcock, G. T., and Yocum, C. F. (1989) Isolation and characterization of the 47 kDa protein and the D1−D2-cytochrome-b-559 complex, *Biochim. Biophys. Acta 974*, 44−53.
40. Tracewell, C. A., Vrettos, J. S., Bautista, J. A., Frank, H. A., and Brudvig, G. W. (2001) Carotenoid photooxidation in photosystem II, *Arch. Biochem. Biophys. 385*, 61−69.
41. Wenk, S.-O., Schneider, D., Boronowsky, U., Jäger, C., Klughammer, C., de Weerd, F. L., van Roon, H., Vermaas, W. F. J., Dekker, J. P., and Rögner, M. (2005) Functional implications of pigments bound to a cytochrome b_6f complex, *FEBS J. 272*, 585−592.

42. Ruban, A. V., Dekker, J. P., Horton, P., and van Grondelle, R. (1995) Temperature dependence of chlorophyll fluorescence from the light harvesting complex II of higher plants, *Photochem. Photobiol. 61*, 216−221.
43. Gobets, B., van Amerongen, H., Monshouwer, R., Kruip, J., Rögner, M., van Grondelle, R., and Dekker, J. P. (1994) Polarized site-selected fluorescence spectroscopy of isolated photosystem I particles, *Biochim. Biophys. Acta 1188*, 75−85.
44. Vladkova, R. (2000) Chlorophyll *a* self-assembly in polar solvent−water mixtures, *Photochem. Photobiol. 71*, 71−83.
45. Palacios, M. A., de Weerd, F. L., Ihalainen, J. A., van Grondelle, R., and van Amerongen, H. (2002) Superradiance and exciton delocalization in light-harvesting complex II from green plants, *J. Phys. Chem. B 106*, 5782−5787.
46. Mullineaux, C. W., Pascal, A. A., Horton, P., and Holzwarth, A. R. (1993) Excitation energy quenching in aggregates of the LHCII chlorophyll-protein complex: A time-resolved fluorescence study, *Biochim. Biophys. Acta 1141*, 23−28.
47. Barzda, V., Gulbinas, V., Kananavicius, R., Cervinskas, V., van Amerongen, H., van Grondelle, R., and Valkunas, L. (2001) Singlet−singlet annihilation kinetics in aggregates and trimers of LHCII, *Biophys. J. 80*, 2409−2421.
48. Vavilin, D. V., Ermakova-Gerdes, S. Y., Keilty, A. T., and Vermaas, W. F. J. (1999) Trytophan at position 181 of the D2 protein of photosystem II confers quenching of variable fluorescence of chlorophyll: Implications for the mechanism of energy-dependent quenching, *Biochemistry 38*, 14690−14696.
49. Peterman, E. J. G., Wenk, S.-O., Pullerits, T., Pålsson, L.-O., van Grondelle, R., Dekker, J. P., Rögner, M., and van Amerongen, H. (1998) Fluorescence and absorption spectroscopy of the weakly fluorescing chlorophyll *a* in cytochrome b_6f of *Synechocystis* PCC 6803, *Biophys. J. 75*, 389−398.
50. Dashdorj, N., Zhang, H., Kim, H., Yan, J., Cramer, W. A., and Savikhin, S. (2005) The single chlorophyll *a* molecule in the cytochrome b_6f complex: Unusual optical properties protect the complex against singlet oxygen, *Biophys. J. 88*, 4178−4187.
51. Kurisu, G., Zhang, H., Smith, J. L., and Cramer, W. A. (2003) Structure of the cytochrome b_6f complex of oxygenic photosynthesis: Tuning the cavity, *Science 302*, 1009−1014.
52. Martin, J. H., Gordon, R. M., and Fitzwater, S. E. (1990) Iron in Antarctic waters, *Nature 345*, 156−158.
53. Thomas, D. N. (2003) Iron limitation in the Southern Ocean, *Science 302*, 565−566.
54. Sarcina, M., and Mullineaux, C. W. (2004) Mobility of the IsiA chlorophyll-binding protein in cyanobacterial thylakoid membranes, *J. Biol. Chem. 279*, 36514−36518.
55. Dekker, J. P., and Boekema, E. J. (2005) Supramolecular organization of thylakoid membrane proteins in green plants, *Biochim. Biophys. Acta 1706*, 12−39.

BI0510680